Int J Appl Earth Obs Geoinformation 61 (2017) 14–21

Contents lists available at ScienceDirect

Int J Appl Earth Obs Geoinformation

journal homepage: www.elsevier.com/locate/jag

Sentinel-1 observations of the 2016 Menyuan earthquake: A buried reverse event linked to the left-lateral Haiyuan fault

H. Wang[a,b,c,*], J. Liu-Zeng[a], A.H.-M. Ng[c,d], L. Ge[d], F. Javed[e,f], F. Long[g], A. Aoudia[e], J. Feng[h], Z. Shao[i]

[a] State Key Laboratory of Earthquake Dynamics, Institute of Geology, China Earthquake Administration, Beijing, China
[b] Collaborative Innovation Center of Geospatial Technology, Wuhan University, Wuhan, China
[c] Department of Surveying Engineering, Guangdong University of Technology, Guangzhou, China
[d] School of Civil & Environmental Engineering, The University of New South Wales, Sydney, Australia
[e] The Abdus Salam International Centre for Theoretical Physics, Earth System Physics Section, Trieste, Italy
[f] Centre for Earthquake Studies, National Centre for Physics, Islamabad, Pakistan
[g] Earthquake Administration of Sichuan Province, Chengdu, China
[h] Earthquake Administration of Gansu Province, Lanzhou, China
[i] Institute of Earthquake Science, China Earthquake Administration, Beijing, China

ARTICLE INFO

Keywords:
InSAR
Sentinel-1
Menyuan earthquake
Haiyuan fault
Fault interaction
Geometric complexity

ABSTRACT

Knowledge on the interaction of active structures is essential to understand mechanics of continental deformation and estimate the earthquake potential in complex tectonic settings. Here we use Sentinel-1A radar imagery to investigate coseismic deformation associated with the 2016 Menyuan (Qinghai) earthquake, which occurred in the vicinity of the left-lateral Haiyuan fault. The ascending and descending interferograms indicate thrust-dominated slip, with the maximum line-of-sight displacements of 58 and 68 mm, respectively. The InSAR observations fit well with the uniform-slip dislocation models except for a larger slip-to-width ratio than that predicted by the empirical scaling law. We suggest that geometric complexities near the Leng Long Ling restraining bend confine rupture propagation, resulting in high slip occurred within a small area and much higher stress drop than global estimates. Although InSAR observations cannot distinguish the primary plane, we prefer the west-dipping solution considering aftershocks distribution and the general tectonic context. Both InSAR modelling and aftershock locations indicate that the rupture plane linked to the Haiyuan fault at 10 km depth, a typical seismogenic depth in Tibet. We suggest that the earthquake more likely occurred on a secondary branch at a restraining bend of the Haiyuan fault, even though we cannot completely rule out the possibility of it being on a splay of the North Qilian Shan thrusts.

1. Introduction

The northeastern margin of the Tibetan Plateau accommodates the convergence associated with India-Asia collision according to a combination of fold-thrust belts and strike-slip faults (Tapponnier and Molnar, 1977; Tapponnier et al., 2001) (Fig. 1). The style of deformation varies from west to east in the region. In the west, the convergence is mainly absorbed by the broadly-distributed NW-SE-trending thrust faults with a shortening rate of ~5 mm/yr measured by GPS (Zhang et al., 2004). While in the east, strain is partitioned between the left-lateral strike-slip Haiyuan fault and the North Qilian Shan thrusts in the north (Gaudemer et al., 1995; Lasserre et al., 2002; Liu-Zeng et al., 2007; Daout et al., 2016a). Based on a simplified geological balanced cross-section Gaudemer et al. (1995), inferred that the Qilian Shan thrusts root on to a south-dipping décollement, which merges with the Haiyuan fault at a depth of ~25 km. Understanding the interaction and deformation partitioning on the thrust and strike-slip faults is essential to estimate the earthquake potential.

The ~1000-km-long Haiyuan fault is the major structure responsible for the eastward movement of Tibet relative to the Gobi-Alashan platform. Its slip rate is still controversial and perhaps spatial-variable from 4 to 8 mm/yr (e.g. Zhang et al., 1988; Li et al., 2009; Duvall and Clark, 2010; Chen et al., 2014; Jolivet et al., 2012; Daout et al., 2016a) to larger than 10 mm/yr (e.g. Gaudemer et al., 1995; Lasserre et al., 1999, 2002). The region around the Haiyuan fault system is one of the most seismically active areas in Tibet with many devastating earth-

* Corresponding author at: Department of Surveying Engineering, Guangdong University of Technology, Guangzhou, China.
E-mail address: ehwang@163.com (H. Wang).

http://dx.doi.org/10.1016/j.jag.2017.04.011
Received 18 October 2016; Received in revised form 15 April 2017; Accepted 23 April 2017

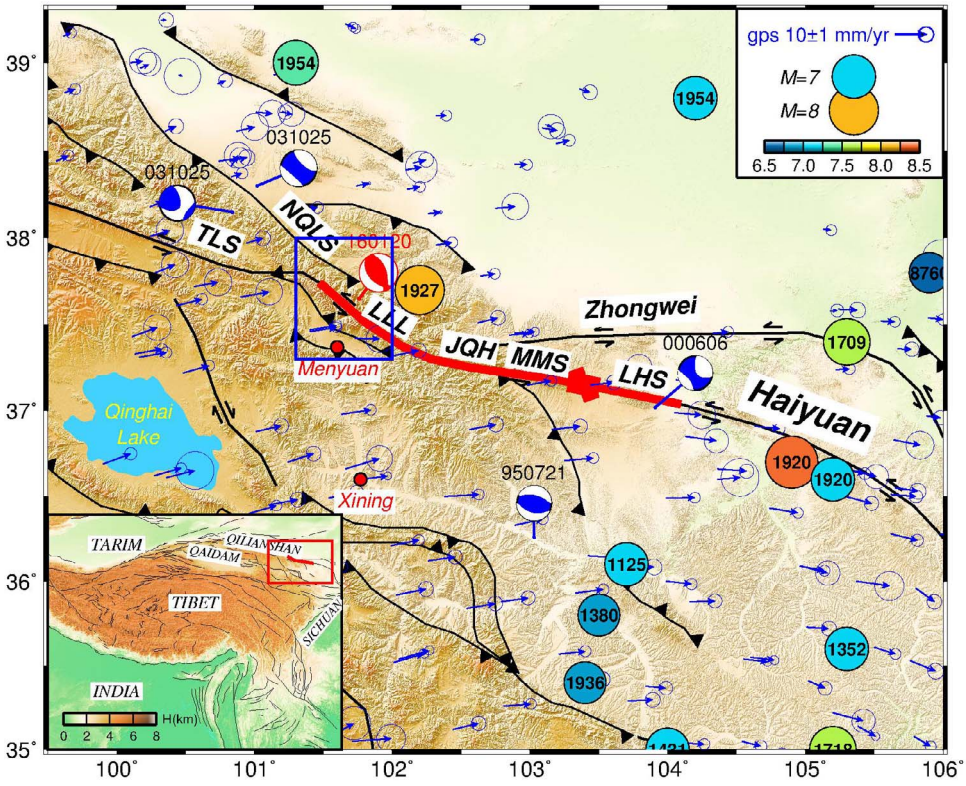

Fig. 1. Tectonic map and historical earthquakes around the Haiyuan fault. The coloured circles with year of occurrence inside denote $M \geq 6.5$ historical earthquakes until 1990 from Gu (1983) and the GCMT catalogue. The blue-white "beach-balls" with dates (yymmdd) on top represent focal mechanisms of the earthquakes since 1991. The 2016 Menyuan earthquake is as a red-white "beach-ball". The active faults are from Taylor and Yin (2009), in which the Tianzu seismic gap is highlighted with a thick red line. The blue box delimits the extents of the interferograms shown in Fig. 2. Abbreviations of the fault names are NQLS – North Qilian Shan, TLS – Tuo Lai Shan, LLL – Leng Long Ling, JQH – Jin Qiang He, MMS – Mao Mao Shan, LHS – Lao Hu Shan. Blue arrows are GPS velocities from Liang et al. (2013). Inset is the topography and active faults in the whole Tibetan Plateau. The red box indicates the location of the major figure, and the red line highlights the Tianzu gap. (For interpretation of the references to color in this figure legend, the reader is referred to the web version of the article.)

quakes, such as the 14 October 1709 M 7.5 Zhongwei, the 16 December 1920 M_w 7.8 Haiyuan and the 22 May 1927 M 7.9 Gulang events (Gu, 1983; Deng et al., 1986; Liu-Zeng et al., 2007). In which, the 1920 earthquake caused severe casualties killing at least 220,000 people (Liu et al., 2003). Between the Haiyuan and Gulang earthquakes, the ~260-km-long segment has been absent of large earthquake over 800 years. It was therefore considered as a seismic gap, namely "Tianzu gap", where may generate $M \geq 7.5$ earthquakes (Gaudemer et al., 1995). The Tianzu gap is composed of four segments from east to west including Lao Hu Shan, Mao Mao Shan, Jin Qiang He and Leng Long Ling (LLL) (Gaudemer et al., 1995).

On 20 January 2016, a M_w 5.9 earthquake occurred in Menyuan county, about 55 km west of the 1927 Gulang earthquake and 110 km north of Xining – the provincial capital of Qinghai. It is the largest since the 26 August 1986 M_w 5.9 earthquake. The epicentre lies between the east end of the North Qilian Shan fault and the west end of the Tianzu gap near the LLL mountain (Fig. 1). The south flank of the LLL mountain range is bounded by north-dipping reverse faults and thus separated from the Tertiary Menyuan basin. Together, the fault system near the Menyuan earthquake resembles a crustal-scale flower-structure. Geometric complexities here might affect the initiation and propagation of the Menyuan earthquake ruptures (King and Nabelek, 1985; Wesnousky, 2006). It is also not clear whether this earthquake signals an increase loading on the Haiyuan fault, or it is an aftershock of the 1927 Gulang earthquake. Its mechanism and structural affinity therefore should shed light on understanding the interaction of active structures and clarifying which fault the earthquake is associated. Although reverse events are common in northeastern Tibet, none of them has been investigated using geodesy except for the 2008/2009 Qaidam earthquakes whilst far from the Haiyuan fault (Elliott et al., 2011). This enhances the importance of the Menyuan earthquake for studying regional tectonics and seismic potential, given that it occurred roughly near the end of the seismic gap. Using Sentinel-1A data, Li et al. (2016) derived coseismic deformation and a dislocation model of the Menyuan earthquake. Here we provide different solutions from similar radar imagery together with aftershock relocation and Coulomb stress changes.

2. InSAR data analysis

We use two pairs of Sentinel-1A radar images acquired in TOPS mode on the ascending track 128 and descending track 033, respectively. These datasets have the shortest temporal and perpendicular baselines available (Table 1). We produce interferograms from the SLC

Table 1
Interferometric pairs used in this study.

Master-slave (yymmdd)	Orbit direction	Track	$B_\perp$ (m)	B_T (day)	Incidence (degree)	σ (mm)	α (km)
160113–160206	Ascending	128	17	24	36–40	5	19
160118–160211	Descending	033	12	24	34–38	3	13